

# Identification of Neutrino Interactions using the DONUT Spectrometer

K. Kodama <sup>a</sup>,  
C. Andreopoulos, N. Giokaris, N. Saoulidou, G. Tzanakos <sup>b</sup>,  
B. Baller, D.Boehnlein, B. Lundberg, R. Rameika <sup>c</sup>,  
J.S. Song, C.S. Yoon, S.H. Chung <sup>d</sup>,  
P. Berghaus, M. Kubantsev, N.W. Reay <sup>e</sup>,  
R. Sidwell, N. Stanton, S. Yoshida <sup>e</sup>, S. Aoki, T. Hara <sup>f</sup>,  
D. Ciampa, C. Erickson, K. Heller, R. Rusack, M. Graham <sup>g</sup>,  
R. Schwienhorst, J. Sielaff, J. Trammell, J. Wilcox <sup>g</sup>,  
K. Hoshino, H. Jiko, J. Kawada, T. Kawai, M. Komatsu <sup>h</sup>,  
H. Matsuoka, M. Miyanishi, M. Nakamura, T. Nakano, K. Narita <sup>h</sup>,  
K. Niwa, N. Nonaka, K. Okada, O. Sato, T. Toshito <sup>h</sup>,  
T. Akdogan, A. Kulik, V. Paolone <sup>i</sup>, C. Rosenfeld <sup>j</sup>,  
T. Kafka, W. Oliver, J. Schneps, M. Skender <sup>k</sup>

<sup>a</sup> *Aichi University of Education, Kariya, Japan*

<sup>b</sup> *University of Athens, 15771 Athens, Greece*

<sup>c</sup> *Fermilab, Batavia, Illinois 60510*

<sup>d</sup> *Gyeongsang University, Chinju, Korea*

<sup>e</sup> *Kansas State University, Manhattan, Kansas 66506*

<sup>f</sup> *Kobe University, Kobe, Japan*

<sup>g</sup> *University of Minnesota, Minnesota*

<sup>h</sup> *Nagoya University, Nagoya 464-8602, Japan*

<sup>i</sup> *University of Pittsburgh, Pittsburgh, Pennsylvania 15260*

<sup>j</sup> *University of South Carolina, Columbia, South Carolina 29028*

<sup>k</sup> *Tufts University, Medford, Massachusetts 02155*

---

## Abstract

The experimental apparatus used for the first direct observation of the tau neutrino (the DONUT experiment) is described. Its main features consisted of a target system composed of nuclear emulsion targets and scintillation fiber trackers, a magnetic charged-particle spectrometer and detectors for lepton identification. This

article will concentrate on the description of the electronic detectors and their performance in selecting neutrino interactions, making the vertex predictions necessary for locating events in the emulsion target and lepton identification.

---

## 1 Introduction

The DONUT experiment was proposed to directly observe charged-current interactions of the tau neutrino,  $\nu_\tau$  (1). The detectors were constructed and installed in the Fermilab PW beamline in 1996. The neutrino data were taken from April 1997 until September 1997. The first phase of the analysis was completed by July 2000 and the observation of four events satisfying the requirements of tau production in emulsion was published (2). This paper describes the design and performance of the electronic, real-time, part of the apparatus.

After a brief overview of the conceptual design in Section 2, each major subsystem is detailed: the target system in Section 3, the magnetic spectrometer in Section 4, and lepton identification in Section 5. Section 6 contains a synopsis of the performance of the electronic detectors as an integrated system for the detection of neutrino interactions. The emulsion was the heart of our experiment, but for this publication it is considered only as a passive target material. The details of the emulsion target design and analysis can be found in a separate paper (3). The electronic detector was also used in the analysis of the tau neutrino magnetic moment where the emulsion was used passively (4).

## 2 Conceptual Design

### 2.1 Prompt Neutrino Beam

The neutrino beam in DONUT was generated primarily by the leptonic decays of charmed mesons, which were produced by 800 GeV protons from the Tevatron onto a 1 m long tungsten beam dump. The main  $\nu_\tau$  source was the decay of the  $D_s$  meson:  $D_s \rightarrow \nu_\tau + \tau$ , where  $\tau \rightarrow (\nu_\tau \text{ or } \bar{\nu}_\tau) + X$ . Approximately 5% of the neutrinos were estimated to be  $\nu_\tau$ , with 58% measured to be  $\nu_\mu$  and 37%  $\nu_e$ . The average neutrino energy was 53 GeV. The other products from the proton interactions had to be greatly attenuated by magnetic and passive shielding so that the residual background of particles at the emulsion could be tolerated during a one to two month exposure. Experience prior to this experiment had shown that the integrated penetrating charged particle track

density through the emulsion had to be limited to less than  $5 \times 10^5$  tracks per  $\text{cm}^2$  (5). The two significant backgrounds from the dump were muons and neutrons. The high-energy muons, with momenta greater than  $20 \text{ GeV}/c$ , were not absorbed but deflected horizontally by sweeping magnets. These magnets created, at 35 m from the beam dump, a zone 1 m across that was almost free of muons. Within this zone, the measured muon rate was  $2 \times 10^4$  per  $10^{13}$  protons-on-target (the typical primary beam rate was  $8 \times 10^{12}$  delivered during 20 seconds in a one minute cycle). The neutron flux was reduced by concrete shielding surrounding the beam dump and the measured rate at the emulsion target was 800 neutrons per  $10^{13}$  protons. The neutron spectrum was consistent with almost all being less than 1 MeV and most less than 1 keV. The systematic study of the source of the muons that passed through the target area was done after commissioning the beamline. It was found that there were two identifiable sources: a large angle component ( $>200 \text{ mrad}$ ) that was refocused by the magnet's flux-return steel, and a small angle ( $<30 \text{ mrad}$ ), high momentum component. These small-angle muons were the result of decays of pions produced from the interactions of the primary proton beam, which were produced upstream of the beam dump. A schematic view of the Prompt Neutrino Beam is shown in Fig. 1. Using measured rates, the following limits on the material in the primary beam were derived: in the final 100 m less than  $3 \times 10^{-4}$  interaction lengths, and for 100 m to 300 m upstream less than  $8 \times 10^{-5}$  interaction lengths. The material was mostly residual air within the vacuum pipe, but the rates also included some interactions of the beam halo in the pipe.

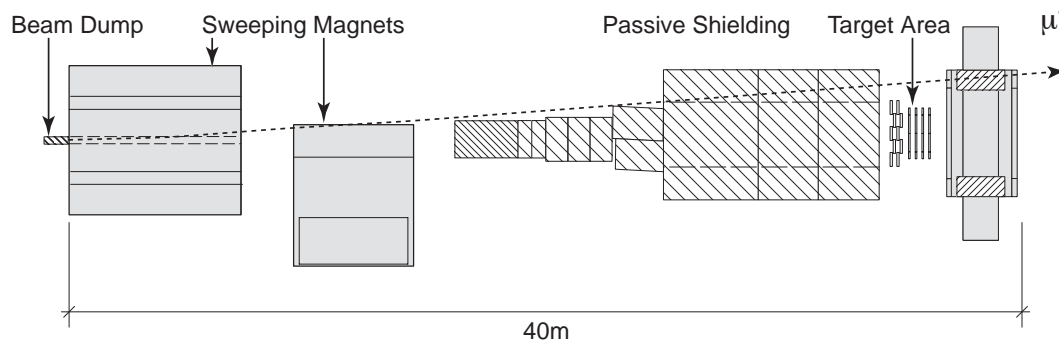


Fig. 1. A schematic view of the Prompt Neutrino Beam. The 800 GeV proton beam was incident from the left. The trajectory of a  $400 \text{ GeV}/c$  muon from the beam dump is shown.

## 2.2 Detectors

Neutrino interactions can be characterized by their mean energy and charged particle multiplicity. Charged current interactions have the added signature of producing a charged lepton of the same flavor as the incident neutrino, whereas

neutral current interactions are characterized by the absence of a charged lepton in the final state. High energy neutrino interactions are typically detected by using high-density target material interleaved with active detectors to measure the energy and direction of the interaction products. Monte Carlo energy and charged particle multiplicity distributions for DONUT neutrino interactions are shown in Fig. 2. The signature for a  $\nu_\tau$  charged-current interaction is the production and subsequent decay of a  $\tau$  lepton. In the DONUT experiment,  $\tau$  leptons produced by  $\nu_\tau$  interactions would have an average decay length of 2 mm with 86% probability of decaying into one charged particle, recognizable by a short track with a kink. The remainder of the decays would be recognized by multi-prong decay topologies. Both of these signatures could only be recognized in DONUT with high resolution emulsion tracking. However, the electronic detectors served four complementary purposes: 1) to selectively trigger on neutrino-like interactions; 2) to reconstruct the triggered events to a level sufficient to reject interactions that were not likely to be from neutrinos; 3) to predict the spatial position of an interaction vertex in the emulsion; and 4) provide lepton identification to distinguish  $\nu_\tau$  interactions from  $\nu_\mu$  and  $\nu_e$  interactions containing an additional track which has the signature of a  $\tau$  decay.

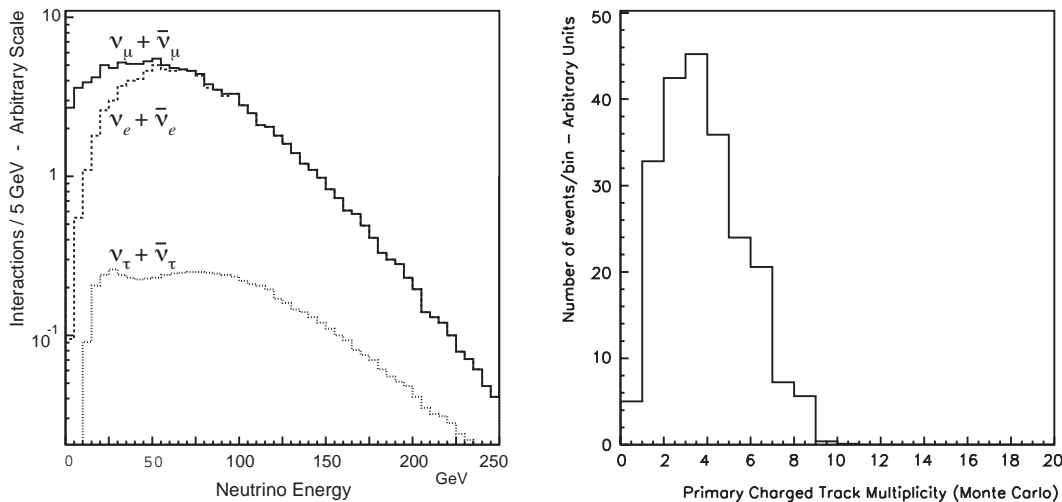


Fig. 2. Monte Carlo distributions of the interacted prompt neutrino energy spectrum for both neutrinos and anti-neutrinos (*left*) and charged-particle multiplicity distributions (*right*) for DONUT neutrino interactions of all flavors.

Emulsion targets, a scintillating fiber tracker (SFT) and trigger counters formed an integrated system which was specifically designed and built for the DONUT experiment. The muon identification system (MID) was also constructed to meet the specific requirements of the beam and physics. However, most of the other elements of the spectrometer, including the drift chambers and the electromagnetic calorimeter (EMCAL), was equipment built for previous experiments, and used again in DONUT. It is important to note that because the emulsion targets were relatively thick (up to 8 radiation lengths down-

stream of the interaction point), most neutrino events could not be fully reconstructed using the spectrometer. Priorities in designing the experiment were to achieve sub-micron precision in the emulsion/SFT and high efficiency in lepton identification. Charged particle tracking in the spectrometer was of lesser importance.

The  $\nu_\tau$  beam was effectively restricted in angular size by kinematics, in that the flux weighted by the cross section was directed forward, with half of the interactions within  $\pm 7.5$  milliradians of the beam direction defined by the protons. Thus, the transverse size of the emulsion target could be scaled with the distance from the beam dump. At the distance of 36 m from the dump, which was necessary for adequate shielding, the transverse size of the emulsion was restricted to  $50 \times 50$  cm<sup>2</sup>. This size subsequently set the scale for the transverse size of the SFT. Finally, the distance from the emulsion to the magnet was set by matching the angular acceptance to the MID. A plan-view schematic drawing of the apparatus is shown in Fig. 3.

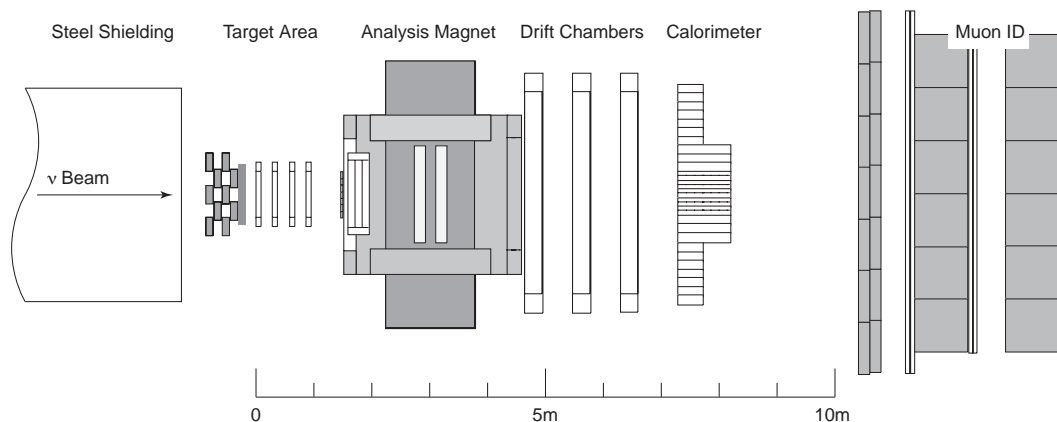


Fig. 3. A plan-view schematic drawing of the DONUT apparatus.

### 3 Target System

The target system was a compact and modular group of detectors including emulsion targets, SFT, and trigger system. The emulsion and the SFT were enclosed in a light-tight and shielded target box, 75 cm  $\times$  75 cm in width and 185 cm long. An important feature in the design of this system was the segmentation along the beam direction. The target box, shown in Fig. 4, contained four separate emulsion modules with a set of SFT planes just downstream of each. The emulsion modules and SFT sets were aligned and mounted on a precision stand. Each emulsion target module had a thickness of 7 cm corresponding to 2~3 radiation lengths. This segmentation along the beam direction was crucial to reconstructing neutrino interaction vertices with the SFT, while providing an adequate target mass.



Fig. 4. The target area with neutrinos incident from left. Shown are the array of veto counters, followed by lead shielding and the stand holding the emulsion and SFT. The entire emulsion/SFT system was encased in a 2 cm thick lead box, one panel of which is removed in this drawing.

### 3.1 Emulsion Targets

Emulsion target modules were made by stacking individual  $50\text{ cm} \times 50\text{ cm}$  emulsion sheets inside separate aluminum support frames. Details of the construction of the sheets is given in Ref. (3). The sheets were oriented perpendicular to the beam. For most of the targets (65%) the emulsion sheets were interleaved with 1 mm thick stainless steel plates. This application of steel-emulsion modules, named ECC (for “Emulsion Cloud Chamber”), was used in DONUT to greatly increase the target mass to emulsion ratio, while maintaining a high efficiency for recognizing  $\tau$  decays. There were a total of seven emulsion modules constructed and exposed during the experiment, with at most four being installed at any time. Two modules were made of entirely ECC type sheets. One module was entirely of the Bulk type (emulsion only), and the remaining four modules were a combination of ECC and Bulk sheets. The masses of the modules ranged from 56 kg (no steel plates) to 100 kg. The beam-weighted average mass of the installed targets was 260 kg. The type of emulsion and mass of each of the modules placed in the target station are listed in Table 3.1. The thickness of the targets implied that for most events secondary interactions would occur within the modules. The target segmentation could be used as a sampling electromagnetic calorimeter for events originating in the first two modules. Detailed discussion of the use of the emulsion as an active target can be found in Ref. (3).

Module	Target Station	ECC Mass (kg)	Bulk Mass (kg)	Total Mass (kg)
ECC1	1	100.49		101.49
ECC3	3	100.49		101.49
E/B1	1	49.15	19.35	69.45
E/B2	2	42.12	25.15	66.70
E/B3	3	44.46	21.28	66.70
E/B4	4	36.71	27.73	67.31
B4	4		56.10	57.06

Table 3.1

Emulsion target masses. There were up to four modules installed at any time, and a total of seven exposed over the duration of the experiment.

### 3.2 Scintillating Fiber Tracker (SFT)

The SFT system provided charged particle tracking downstream of each emulsion module. There were four separately mounted stations, each containing 9 to 13 planes of scintillating fibers. Using hits in the SFT, tracks could be reconstructed for making predictions of the interaction vertex within the emulsion module. The SFT and its readout were based on the design used in the CHORUS experiment (6).

There were  $6 \times 10^4$  scintillating fibers in the SFT. The fibers were Kuraray SCSF78, 500  $\mu\text{m}$  diameter. The fiber length varied between 0.7 m and 1.2 m. Light from the fibers was read out at one end, and the other end was aluminized. The fibers were continuous (one piece) to the readout bundles, which simplified construction without serious loss of light.

The fibers were arranged in layers, with 1200 fibers per layer. Each layer was coated with reflective  $\text{TiO}_2$  loaded paint that also served as a glue. Each plane had an area of 0.56 m  $\times$  0.56 m. The fiber planes were arranged to measure coordinates  $u$ ,  $v$ , and  $x$ . The  $u - v$  axes were oriented at  $45^\circ$  to the  $x - y$  axes, where the  $y$  axis was vertical. The  $u$  and  $v$  planes each had two layers of fibers; the  $x$  planes had four. There were 44 planes of fibers altogether, in four stations downstream of each emulsion module: 4  $x$  planes, 20  $u$  planes, and 20  $v$  planes. The configuration of the SFT planes is shown in Fig. 5.

The fibers were bundled and stacked to a rectangular geometry for readout by six image intensifier units (IIT). The IITs produced an amplified image of the bundled fibers that was digitized by a CCD camera. There were four stages in each IIT that provided a maximum gain of about 40 per stage, for

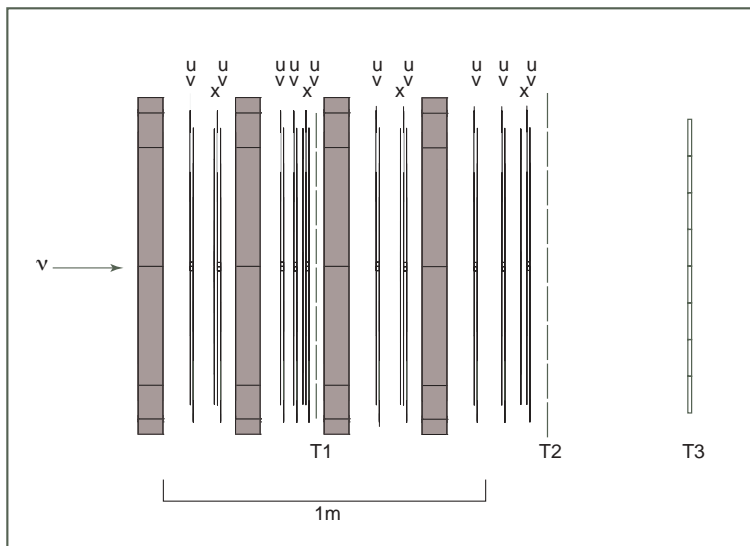


Fig. 5. Plan view of the SFT planes and trigger counters. The emulsion modules are shaded.

a total gain of about  $3 \times 10^6$ . The sensitivity of the third stage was normally kept low by maintaining the accelerating potential 6 kV below the normal operating condition of 20 kV. Upon receiving a trigger signal, this voltage was quickly increased, and the IIT stage became fully efficient. The slow phosphor of the photocathode and gated voltage, allowed the trigger electronics the time needed to make a decision to keep or reject the event.

Because the IITs are imaging tubes, they are very sensitive to magnetic fields. The image was significantly distorted for field changes as small as 0.1 gauss. The proximity of the spectrometer magnet, about 1 m, required that each IIT be surrounded by heavy iron shields in addition to high-permeability inner shields. The image of the fiber bundle from the IIT was demagnified and focussed onto a  $8.8 \text{ mm} \times 6.6 \text{ mm}$  ( $768 \times 493$  pixels) CCD camera module. The signal from each pixel of the CCD was digitized by an 8-bit flash ADC. The pixels above a set threshold were read out at a rate of 14 MHz. The mean time to read out a single event from the CCD camera was 24 ms, which was, by far, the major component of the data acquisition dead-time. CCD data were stored in a VME-based memory.

The alignment of the image of the fiber bundle was a critical process in using the SFT data. Each circular fiber was mapped onto an area corresponding to  $3 \times 3$  pixels on the CCD. A complete map of pixels to fibers for each IIT was greatly aided by illuminating every twelfth fiber during special calibration events, which were taken every minute. The illuminated fibers formed a fiducial grid, which was analyzed for each run, allowing the SFT data to be corrected systematically. The SFT planes were aligned with the other components of the spectrometer using muons from the beam dump that penetrated the whole apparatus. Both the position and light output were recorded for

every fiber above the pixel readout threshold. The pulse height could discriminate between minimum ionizing particles and larger energy losses due to either slow particles ( $\propto v^{-1}$ ) or electrons with an  $e^+e^-$  pair within the 0.5 mm fiber width. Thus, for SFT hits associated by linking into tracks, the identity of slow hadrons, or electrons (either from the primary interaction or  $\pi^0$  decay) could be made with high probability. The SFT resolution and efficiency are listed in Table 4.3.

### 3.3 Trigger System and Data Acquisition System

The electronic detectors required a prompt trigger for the digitizing and read-out electronics. A simple and efficient trigger for recording neutrino interactions required that no charged particles entered the emulsion from upstream and at least one charged particle emerged from an emulsion target. This trigger was formed by a series of scintillation counters consisting of a veto wall upstream of the emulsion target stand and three hodoscope planes distributed between and downstream of the emulsion modules. The veto wall consisted of 10 counters and covered a total area of 140 cm  $\times$  152 cm. The dimensions of each counter were 30.5 cm in  $x$ , 152 cm in  $y$ , and 10 cm in  $z$ . In order to maintain high efficiency for detecting penetrating charged particles, the wall was arranged in two layers along  $z$ . For muons, the veto wall efficiency was determined to be better than 99.9%.

Two planes of scintillating fibers, T1 and T2, were located downstream of the 2nd and 4th target modules respectively. Each plane was 70 cm  $\times$  70 cm in area and segmented into eight (T1) or nine (T2) 10 cm bundles. Each bundle was read out by a Hamamatsu R5600 phototube. A scintillator hodoscope, T3, was located downstream of the target/SFT box. It was composed of eight counters, each 10 cm  $\times$  80 cm and 5 mm thick. Each counter had 49 cm long light guides and a phototube (Philips 2262B) attached at both ends. All counters exceeded 96% in efficiency for muons.

Two triggers were used during the course of the experiment. The design goal of the trigger system was to keep data acquisition live time at greater than 85%, which would correspond to a trigger rate of 6 Hz. The main trigger (Trigger A) required: (1) hits in T1, T2 and T3 consistent with  $\geq 2$  charged tracks; (2) track angles  $> 250$  milliradians; and (3) no hits in the veto wall. Hits in the counters were input to Memory Lookup Units (MLU) and patterns of hits meeting the three requirements initiated a trigger pulse from the MLUs. Trigger A was the sole physics trigger for the first 53% of the recorded data. The fact that it required more than one charged particle compromised the efficiency for triggering on single multiplicity neutrino interactions. This compromise was necessary since the trigger rate for a single track was very

high due to background processes initiated by through-going muons from the dump. Because of the limited speed of the SFT readout system, discussed above, the live-time of the experiment would have dropped far below the design goal. The measured average rate for Trigger A was 4.5 Hz corresponding to a live-time of 90%.

During the final 6 weeks of data taking (47% of the recorded data), a second trigger (Trigger B) was implemented in order to include single track interactions that were lost in Trigger A. This trigger used the MLUs to require a proper 1-track pattern and, in addition, required at least one minimum ionizing track in the electromagnetic calorimeter. The input from the calorimeter did not include the sections of blocks that had high counting rates from the muons swept to either side of the target. With the addition of Trigger B, the trigger rate increased to 5.5 Hz and the live-time decreased to 87%.

The efficiency of the triggers for neutrino interactions was calculated using simulated events with actual geometries and measured efficiencies for each counter. It was estimated that the efficiency was 98% for triggering on charged-current neutrino interactions of electron- and muon-neutrinos, 84% for neutral-current interactions, and 97% for  $\nu_\tau$  interactions.

The data acquisition system (DAQ) collected the data from the digitizing electronics for each detector, stored it in a buffer, and after the beam pulse, wrote the data onto magnetic tapes. The architecture of the DAQ was based on the Fermilab DART product (7), using VME-based microprocessors to control the transport of data from the VME buffers to a host computer. The host computer served as both the data monitor and as the data logger to tape (Exabyte 3500). The average event size was 100 kB, with a throughput of 10 MB per beam cycle of one minute.

## 4 Magnetic Spectrometer

The magnetic spectrometer consisted of a large aperture dipole magnet, located between two sets of drift chamber tracking detectors. It served three main functions, which were, in order of importance: (1) to measure the momentum of muons from neutrino interactions; (2) to cross-check the momentum measurement for a sample of tracks whose momenta were measured both in the spectrometer and by multiple scattering in the emulsion; and (3) to cross-check the calibration of the EMCAL with momentum analyzed electron tracks from interactions. Less than 20% of the interactions could be fully reconstructed using the spectrometer, and these events were strongly biased to low multiplicity, muon-neutrino charged-current events.

### 4.1 Magnet

The spectrometer magnet was a wide-aperture dipole. The rectangular (air) gap measured 70 cm high and 150 cm wide. There were 20 cm thick “mirror” plates mounted on both ends to reduce the magnetic field outside of the coils. The central field maximum was 4 kG and the  $\int B \cdot dl$  along the central (beam) axis was 0.75 kG m (equivalent to 225 MeV/ $c$   $p_T$  kick). The  $B$  field was mapped, using a 2cm grid, over the entire aperture to an accuracy of  $< 1\%$  per point and 3% to the integrated field along tracks.

### 4.2 Vector Drift Chambers

The upstream aperture of the spectrometer magnet held three drift chambers (VDC1-3), all of the “vector” or “jet” chamber design, with each cell having many sense wires spaced along the beam direction. The first chamber’s gas volume contained three vector planes, with vertical sense wires in the first plane and wires offset at  $\pm 4.2^\circ$  for the second and third planes. The cells, 16 total, measured 7 cm wide and 9 cm in depth with six sense wires. These planes had an effective active area of 70 cm high  $\times$  100 cm wide. These chambers were designed for and used in a previous fixed target experiment and described in more detail in Ref. (8).

The next two planes of vector drift chambers were designed and built specifically for DONUT. Each was mounted in a separate volume about half the distance through the magnet aperture. The first plane had horizontal sense wires, with 16 cells of 6.6 cm width, and four samples along the beam. The second chamber had 22 cells of the same design, but the wires were oriented vertically. All three vector chambers used a gas mixture of 80% Ar and 20% CO<sub>2</sub>, and all wires were read out through LRC 3377 multi-hit TDCs (444 channels total).

### 4.3 Large Aperture Drift Chambers

Three large-aperture drift chambers (DC4-6) of conventional (one sense wire per cell) design were situated between the magnet and the EMCAL. Each chamber housed four planes: two with vertical wires, and two at  $\pm 16.7^\circ$  from vertical. These chambers were used in several previous experiments and are described in Ref. (9). The spacing between sense wires was 0.95 cm. The first chamber was instrumented to give an active area of 1.6 m  $\times$  2.2 m, the second and third had an active area of 1.6 m  $\times$  3.3 m. The DC’s were operated with a 50-50 Argon-Ethane gas mixture and were read out using LeCroy 4291 TDC’s

in a common stop mode. Resolution and efficiency for both the VDC and DC systems are listed in Table 4.3.

Detector	Resolution ( $1 \sigma$ )	Efficiency
SFT ( $u/v$ planes)	170 $\mu\text{m}$	96%
SFT ( $x$ planes)	170 $\mu\text{m}$	>99%
VDC1-3	180 $\mu\text{m}$	96%
DC4-6	320 $\mu\text{m}$	88%

Table 4.3  
Resolution and efficiency of tracking detectors.

## 5 Muon and Electron Tagging

Efficient identification of leptons was crucial for the reduction of background in tau-neutrino interactions. The kink signature of an emulsion track may be from a  $\tau$  lepton decay provided that there are no other leptons produced at the primary vertex. The rejection of charm decays, topologically similar to tau decays, is the main purpose of the lepton identification systems.

### 5.1 Electron Tagging

Electrons were tagged in the DONUT analysis with three techniques, depending on the location of the interaction vertex.

- (1) Electrons that passed through 2 or more radiation lengths in the emulsion targets could be identified using emulsion data, by electron pair tracks in proximity to the primary track;
- (2) Electrons that originated in the two upstream target modules could be tagged by their associated showers seen in the SFT, which develop in the remaining downstream modules. By counting hits and using the longitudinal development of the cascade, an estimate for the initial electron energy could also be derived.
- (3) Electrons that originated in the third and fourth target modules could be tagged using the EMCAL. The electronic detectors provided the data for the analysis of the second and third methods. An example event showing the characteristics of an electron shower is shown in Fig. 6.

The EMCAL was a 400 element array of lead glass and scintillating glass which was designed and built for a previous experiment which ran in the PW beamline and is described in detail in Ref. (10). Its transverse dimensions

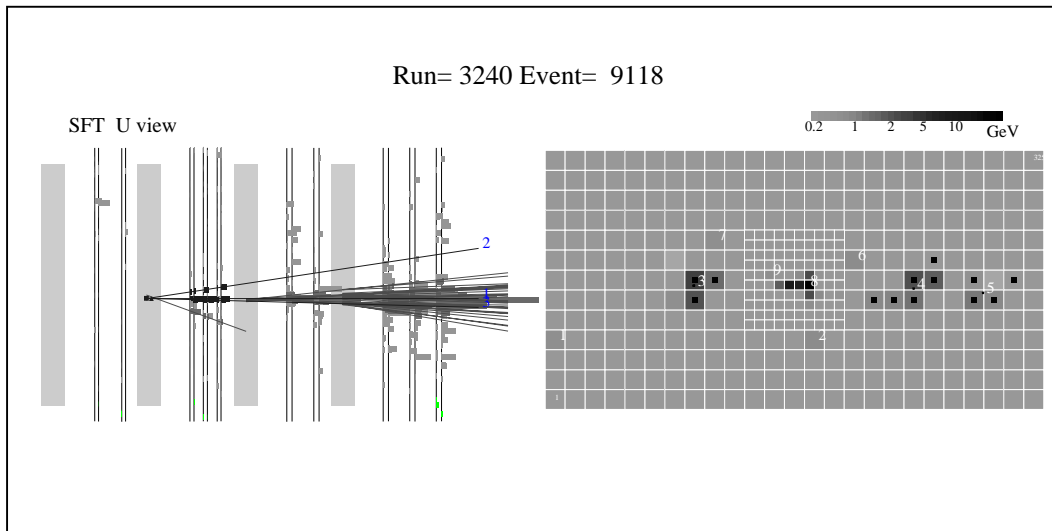


Fig. 6. Electron tagging was done using shower development in the Emulsion/SFT system (*left*) and by using energy clusters in the calorimeter (*right*). The same event is shown in both systems. A neutrino interaction in the second emulsion module produces an electron that showers in the next two modules. The energy deposition in the calorimeter blocks is characteristic of an electromagnetic cascade dispersed horizontally after the analyzing magnet.

were 1.95 m high  $\times$  3.75 m wide. The central region was composed of SCG-1 scintillating glass blocks, 7.5 cm  $\times$  7.5 cm  $\times$  89 cm, while the outer regions were made of 15 cm  $\times$  15 cm  $\times$  89 cm scintillating glass blocks and SF5 lead glass blocks, 43 cm long. The small blocks were read out by RCA6342A photomultipliers and the large blocks were read out by EMI-9791 photomultipliers. The signals from the PMTs were split so that most of the signal, 80%, was digitized by ADCs (LRS 2280 system, 15-bit). The remaining 20% of the signal was discriminated and used for Trigger B, discussed above. The PMT gain was continuously monitored by an LED pulser used with 0.3 mm optical fibers to distribute the light to the front of each block. The LED system stability was within 2% throughout the experiment.

A sample of blocks, including all three types, was tested in a beam at Brookhaven National Laboratory before the data run at Fermilab. The blocks were exposed to electrons, pions and muons. This test established the ratio of the muon response to electron response. This was necessary since there was no means of delivering a calibration beam to the EMCAL once it was installed in DONUT. During the run, the well-measured ratio of muon to LED response provided the way to carry the test beam calibration to the entire array and adjust for any changes in response during the data run (13). Although the resolutions of all blocks was better than  $12\%/\sqrt{E}$  in the test beam, it was expected that the response of the whole array would be approximately  $20\%/\sqrt{E}$ . This estimate was checked by using the  $E/p$  ratio for individual tracks in the interaction data, with the result of  $(20 \pm 5)\%$ .

The information from the SFT and the EMCAL is complementary for electron tagging. Tracks originating in the upstream two modules can be efficiently identified in the SFT, but deposit little energy in the EMCAL, while the opposite is true for electrons originating in the two downstream modules. In the analysis, any tracks tagged as electrons in the spectrometer, by either method 2) or 3) were checked in the emulsion data for additional tagging by the  $e^+e^-$  pairs from bremsstrahlung conversion. The efficiency of identifying electrons in the emulsion depended on the path length in emulsion, and is measured to be 85% for lengths of at least  $2X_0$ .

## 5.2 Muon Identification

The muon identifier (MID) tagged muons solely based on range. It was a three-layer array of steel walls and planes of detectors. The upstream wall was 3.7 m high, 6.25 m wide and 0.42 m thick. The second and third walls were each 3.25 m high, 5.48 m wide and 0.91 m thick. The gaps between the walls were approximately 80 cm. Muons greater than 4 GeV pass through all three walls. Proportional tube detector planes were set behind each steel wall, covering 80% of the area, in an ‘‘H’’ configuration. The area cutout of the proportional tubes was where the high momentum muons swept from the dump passed through, as shown in Fig. 7. (Scintillator hodoscopes were built and installed to cover these high rate regions but their performance was poor and the data from these detectors has not been used in the analysis.)

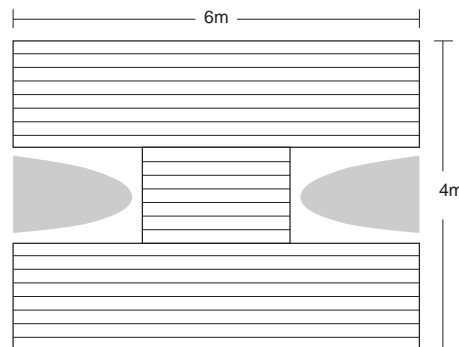


Fig. 7. Geometry of muon identifier proportional tube planes. The regions of high muon flux are shown as shaded areas.

The proportional tubes were made using four-cell aluminum extrusions. Each cell was a square 4 cm on a side. A total of 248 extrusions (992 cells) were made with lengths ranging from 1.3 m to 6.25 m. The tubes were operated with a gas mixture of 95-5% Ar-CO<sub>2</sub>. Each cell contained a 60  $\mu$ m sense wire.

The efficiency of the proportional tubes was measured using muons from the beam dump. A ‘‘hit’’ in MID was defined as a proportional tube hit occurring within 10 cm of the track projection from the DC’s. A track was tagged as a

muon if it had hits in 4 out of 6 possible planes with at least one hit in each of the three walls. The overall efficiency of the system was found to be 93%. The inefficiency is attributed to the relative area of the material between the cells of the extrusions and dead tubes (2%). The total efficiency of the MID, including acceptance and performance was 73.5% for  $\nu_\mu$  charged-current interactions.

## 6 System Performance

### 6.1 Neutrino Interaction Selection

A total of  $6.6 \times 10^6$  triggers for  $3.6 \times 10^{17}$  protons on target were recorded onto tape. However, from calculations, only about  $10^3$  neutrino interactions were expected for this proton exposure. This implied that the great majority of the triggers were background processes satisfying the simple trigger requirements of Section 3.3. Data from the electronic detectors were used to extract the neutrino interaction candidates in a three-step process:

- (1) In the first step, data from the SFT and from the drift chambers were used to reconstruct tracks and to search for a vertex near one of the emulsion targets. This filter reduced the number of events by a factor of 300.
- (2) In the second step, the filtered triggers were examined individually by a physicist using graphical display software. This stage rejected events originating from particle showers produced by high-energy muons and checked for errors in reconstruction and other pathologies. About 90% of the events were rejected quickly and with high confidence. This visual scanning reduced the data by another factor of 20, yielding 898 interaction candidates.
- (3) In the third step, each candidate had an improved vertex position computed for emulsion scanning at Nagoya University. Details regarding this event selection can be found elsewhere (11; 12).

The efficiency of the first step, filtering the raw triggers, was estimated using Monte Carlo simulations. The Monte Carlo events were passed through the filtering code in the same way as the experimental data, except that the simulated data skipped the decoding of the digitizing electronics. The efficiency of the second step, visual scanning, was estimated by comparing results from at least two scanners, and re-scanning data sets by the same scanner. The simulations of neutrino interactions in the detectors took into account the important limitations of the hardware and electronics including: efficiencies, limited hits per cell in the drift chambers (TDC dependent), pulse height dependence on ionization in the SFT, and threshold effects in the trigger counters. The effi-

ciencies for the triggers (including live-time), filtering and visual scanning for  $\nu_\tau$  charged-current interactions are listed in Table 6.1.

Process	Efficiency
Trigger A	96 %
Trigger B	2.4 %
Trigger A or B	97.2 %
Off-line Filter	96 %
Visual Scanning	78 %

Table 6.1  
Summary of Event Selection Efficiencies.

The estimated total efficiency for finding a tau neutrino interaction vertex with the electronic detectors is 73%. These numbers represent the probability that an interaction will be in the emulsion volume that is scanned, but does not include the probability of locating the event in the emulsion, nor finding a kinked track.

## 6.2 Vertex Prediction

A neutrino interaction identified in the electronic detectors by the process described above, must be located in the emulsion target by searching for a vertex within a relatively small volume of digitized emulsion data. The speed of the emulsion scanning stations set practical limits on the volume scanned for each event prediction. The average search volume measured  $5 \text{ mm} \times 5 \text{ mm} \times 15 \text{ mm}$ . In principle, the resolution of the SFT was sufficient to provide a vertex position estimate to much greater precision than this. However, the thick emulsion targets made such predictions much more challenging due to scattering, secondary interactions, and photon conversions. For events with more than five tracks visible in the SFT, the probability of finding a unique match of  $u$ ,  $v$ , and  $x$  hits to form space tracks decreased rapidly with multiplicity. This was partly due to having only one  $x$  plane per station so that the number of  $(u, v)$  combinations matching  $x$  hits was often overwhelming. For events with electromagnetic cascades already developed, the large number of tracks in the SFT make it impossible to reconstruct tracks. These factors required that the method used to estimate the vertex position depended on the characteristics of the SFT data for each event. These classes and characteristics are listed in Table 6.2.

Class 1 events allowed direct computation of vertex position and error, and gave the most accurate results. Class 2 events abandoned three-dimensional fitting, and the vertex solutions in the  $u$  and  $v$  planes were weighted using

Class	Characterization	Method
1	low multiplicity, at least 2 space tracks	vertex fit in space
2	> 5 tracks, some secondary tracks	vertex fit in 2 planes
3	tracking problematic, shower tracks	vertex estimated by clustering

Table 6.2

Classification of SFT Data.

empirically determined parameters to give the  $z$ -position estimate of the vertex. Only a few Class 3 events remained in the data set for location in the emulsion, most were deferred. Examples of SFT data for events from these three classes are shown in Fig. 8. The accuracy of the vertex position for the transverse ( $u, v$ ) and along the beam ( $z$ ) was measured for events located in the emulsion (where the interaction vertex is known to high precision), and is shown in Fig. 9. Note that both the neutrino interaction selection and the vertex prediction did not have any selection criteria specific for  $\nu_\tau$  interactions.

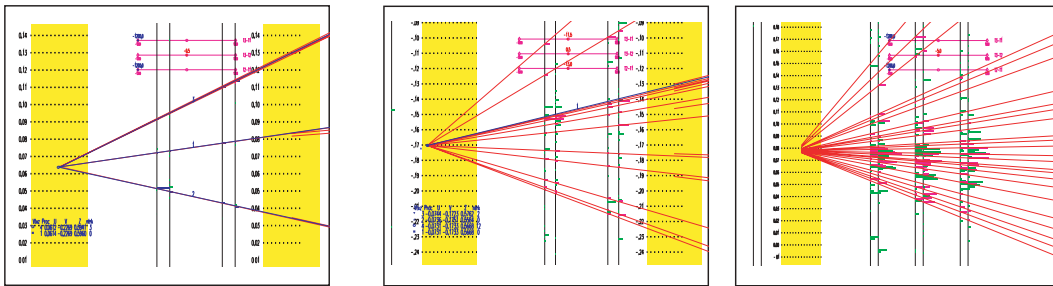


Fig. 8. Examples of the three classes of events, from simple to complex: Class 1 (*left*), Class 2 (*center*), Class 3 (*right*). In each event, the emulsion modules are shaded and track candidates are made from SFT data, shown as lines emerging from the interaction vertex. In Class 3 events, space tracks cannot be uniquely constructed due to the large number of combinations of tracks in each view. For illustrative purposes only, the numbers and labels can be ignored.

### 6.3 Lepton Identification

The overall efficiency for identifying electrons was determined by a Monte Carlo calculation and an exposure of an ECC-type target at KEK using tagged electrons in a test beam. The geometry-specific efficiencies from shower development and acceptance were also calculated using Monte Carlo methods. An overall efficiency for tagging in emulsion for a given depth was derived from the test beam results. Combining both studies gave the efficiency for identifying electrons as  $(70 \pm 3)\%$ .

The efficiency for identifying muons in DONUT was determined by the geometrical acceptance of the proportional tube walls. This depends on the

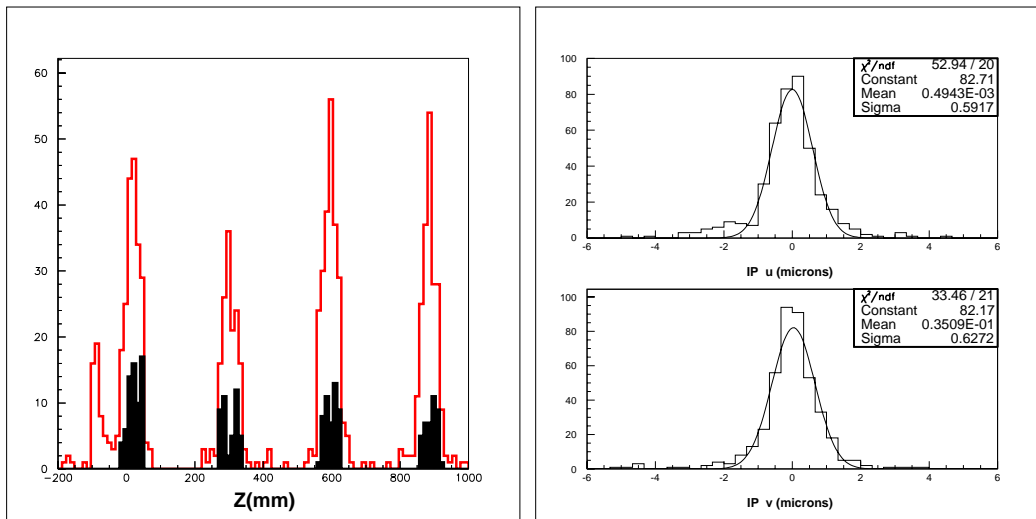


Fig. 9. Vertex predictions and measured location in the emulsion. The left plot shows the longitudinal distribution of vertex predictions (open histogram) and located vertices (filled). Right, the transverse distribution of residuals for located events.

kinematics of the interaction, and hence the incident neutrino flavor. For  $\nu_\mu$  charged-current interactions from a charm meson source in the dump, the efficiency is 72%. For  $\nu_\tau$  charged-current interactions (and subsequent  $\tau$  decay) the efficiency was calculated to be 70%.

## 7 Summary

In the DONUT experiment, the primary role of the electronic spectrometer was to select neutrino interaction candidates and estimate the position of interaction vertex in the emulsion, prior to digitizing the emulsion data. The overall efficiency for these processes was 73% for tau neutrino interactions.

## 8 Acknowledgements

We would like to thank the support staffs at Fermilab and collaborating institutions. We acknowledge the support of the U.S. Department of Energy, the Japan-US Cooperative Research Program, the Ministry of Education, Science and Culture of Japan, the General Secretariat of Research and Technology of Greece, and the Korean Research Foundation and the DOE/OJI Program.

## References

- [1] Fermilab Proposal 872: Measurement of  $\tau$  Lepton Production from the Process  $\nu_\tau + N \rightarrow \tau + X$ , June 1993.
- [2] K. Kodama et al., DONUT Collaboration, Phys. Lett. B 504 (2001) 218.
- [3] K. Kodama et al., DONUT Collaboration, Detection and Analysis of Tau Neutrino Interactions in the DONUT Emulsion Target, submitted to Nucl. Instr. and Meth.
- [4] R. Schwienhorst et al., DONUT Collaboration, Phys. Lett. B 513 (2001) 23.
- [5] K. Kodama et al., E653 Collaboration, Nucl. Instr. and Meth. A289 (1990) 146.
- [6] P. Annis et al., CHORUS Collaboration, Nucl. Instr. and Meth. A 367 (1995) 367.
- [7] G. Oleynik et al., Proceedings of the Conference on Real-time computer applications in nuclear, particle and plasma physics, Vancouver 1993, p. 348.
- [8] M.R. Adams et al., E665 Collaboration, Nucl. Instr. and Meth. A291 (1990) 533.
- [9] T. Alexopoulos et al., E771 Collaboration. Nucl. Instr. and Meth. A 376 (1996) 375.
- [10] L. Antoniazzi et al., E705 Collaboration, Nucl. Instr. and Meth. A 332 (1993) 57.
- [11] R. Schwienhorst, Ph.D. Thesis, University of Minnesota, Minneapolis, MN, May 2000.
- [12] P. Berghaus, Ph.D. Thesis, Kansas State University, Manhattan, KS, 2001.
- [13] N. Saoulidou, Ph.D. Thesis, University of Athens, Greece (in preparation).